Vol.2, No.6, Page 546- 556, 2024 https://doi.org/10.59628/jast.v2i6.1405 ISSN 2958-9568 JAST

SUN PUBLISHER

مجلة جامعة صنعاء للعلوم التطبيقية والتكنولوجيا

Sana'a University Journal of Applied Sciences and Technology

https://journals.su.edu.ye/index.php/jast/

Structural Interpretation of the Aeromagnetic Data Anomalies on the Eastern Part of Sana'a Basin, Yemen

Ahmed A. Alaydrus *, Mohammed A. Mokaber, Manal A. Al-Sharai, Riyadh G. Al-Dheeb and Osamah A. Al-Rool

[1] **Department of Geological Science, Faculty of Petroleum and Natural Resources, University of Sana'a, Sana'a, Yemen.**

*Corresponding author:a.alaydrus@su.edu.ye

Abstract

The studied area is located in the east of Sana'a, Yemen, between latitudes 1700000 - 1720000 N and longitudes 430000 - 450000 E. Geological and aeromagnetic maps of the region (Sheet 13G, scaled at 1:250,000) are among the data used. By analyzing the available aeromagnetic data, the current work seeks to comprehend the regional subsurface structures and their contributions to surface geological formations. A number of analysis methods, such as regional/residual separation, spectral analysis and Euler deconvolution have been used to critically interpret the aeromagnetic map. According to the findings, two tectonic events have primarily influenced the region throughout its geological past. The region's tectonic framework Is largely determined by the tectonic activity of the late Precambrian (Najd Rift System, trending from NW to SE), which has experienced reactivation along with the opening of the Red Sea. Another more recent tectonic event (during the Cenozoic, trending from NE to SW) is linked to the emplacement of a trap volcanic chain and the opening of the Red Sea and the Gulf of Aden. 2D spectrum analysis and 3D Euler deconvolution techniques were used to calculate the depth of the magnetic anomaly sources, which were determined to be between less than 250 and 3086 m.

Article Info

Keywords:
Bani Hushaysh, Aeromagnetic data, RTP, Red Sea, Gulf of Aden

Article History:
Received: 18-November-2024,
Revised: 22-November-2024,
Accepted: 20-December-2024,
Available online: 31 December 2024.

1. INTRODUCTION

The Sana'a Basin is one of Yemen's most important sedimentary basins, characterized by geological and tectonic complexity. Its stratigraphic sequence spans from the Precambrian to the Quaternary, reflecting its significant role in the tectonic system of the Arabian Peninsula. The basin has undergone major tectonic phases during the Jurassic, Cretaceous, Tertiary, and Quaternary periods, influenced by events such as the openings of the Red Sea and Gulf of Aden. These phases have led to uplift, subsidence, and structural reactivations, forming features like anticlines, half-grabens, and volcanic intrusions. Faults, fractures, and tectonic geoformations in the basin highlight the geodynamic processes that have shaped its sedimentary and basement rocks over several geological eras [1]. From the Jurassic to the Quaternary, the geologic succession that outcrops or is subsurface in the greater Sana'a basin can be categorized into three main groups: Quaternary sedimentary rocks, Tertiary trap volcanic sequence, Mesozoic and Paleocene sedimentary formations [2]. This document's discussion of regional aeromagnetic and gravity data emphasizes the importance of mapping tectonic structures using various geophysical techniques. Because they may be interpreted at different scales and efficiently image distinct crustal levels, aeromagnetic and gravity data are strong instruments for tectonic studies. Magnetic data enhance gravity data by detecting structural characteristics and anomalies, whereas gravity data, in particular, offer insights into crustal architecture. These techniques are very useful for structural and tectonic research because they assist in constraining tectonic settings, kinematics, and mineral systems when combined with geological context, suggesting structural mapping techniques, such

as seismic data to image tectonic structures, followed by potential field methods (gravity), which offer insights into crustal density contrasts. Finally, magnetic methods have been employed to refine interpretations, detect igneous intrusions, and identify regional anomalies linked to tectonic processes [3]. In recent years, aeromagnetic surveys have emerged as a vital tool for investigating tectonic structures in sedimentary regions such as the Sana'a Basin. These surveys detect variations in the Earth's magnetic field caused by the distribution of magnetic minerals within the subsurface rocks. By analyzing magnetic data, researchers can identify faults and fractures that are often undetectable using traditional geological methods. Furthermore, aeromagnetic surveys facilitate the identification of subsurface structures that influence tectonic activity, thereby providing valuable insights into the geological framework of the area [4]. Finding the subsurface geological setting using variations in the earth's magnetic field that manifest as anomalies due to the difference in magnetic susceptibility between the basement complex and the sedimentary cap is the primary goal of an aeromagnetic survey. For example, the Sana'a basin shows significant changes in magnetic field signatures, indicating that there are extensive crustal deformations beneath the basin [5]. The Interaction of tectonic activity with aeromagnetic data is crucial in geophysical studies. Tectonic processes can induce significant changes in the magnetic properties of geological structures. These changes manifest as anomalies in the Earth's magnetic field, which can be detected and mapped using aeromagnetic surveys. Tectonic movements may create or alter geological formations, leading to variations in magnetization within the Earth's crust. These variations produce distinct patterns in the magnetic field, which are captured by aeromagnetic surveys conducted from airborne platforms. By analyzing aeromagnetic data, researchers can identify magnetic anomalies associated with fault zones, fractures, and other tectonic features. The integration of aeromagnetic data with tectonic studies allows for the detection and mapping of subsurface structures influenced by tectonic activity. By correlating aeromagnetic anomalies with known tectonic features, researchers can gain insights into the geological history, structural complexity, and potential seismic hazards of a region. This integrated approach enhances our understanding of the Earth's dynamic processes and aids in geological exploration and resource assessment [6]. Therefore, the aim of this study is to utilize aeromagnetic structural features between (1700000 and 1720000 N and 430000–450000E) in the Sana'a Basin in order to provide a more complete view of subsurface geological formations. The research area is located in the Bani Hushaysh District, Sana'a Governorate. It is located approximately 20 km east of Sana'a city and covers an area of 553.6 km2. It is located on a mountainous plateau of sedimentary and volcanic rocks, with numerous valleys such as Wadi Sarrar, Wadi Al-Hais, and the Al-Qasair channel. The area is characterized by high terrain, with a height ranging between 2600 m, at the top of the mountain range in the south of the area, up to 2000 m in the valleys, and agricultural plains located to the west of the study area (Fig. 1) The study area includes mountainous terrain such as Jabal Aiban and Jabal Al-Asbahi, which are high areas that affect the movement of water and direct it towards the plains. Many small valleys that descend from the mountainous areas towards the lowlands are spread out, and the most important of these valleys are:

- Wadi Al-Khader: One of the main valleys in Bani Hushaysh flows towards the plains.
- Wadi Al-Batha: Another valley that contributes to collecting rainwater and feeding agricultural areas. The agricultural areas of the directorate are rich in agricultural lands in the lowlands, where water is collected due to rain and feeds. The low terrain is located in plain areas and depressions that help in collecting water and distributing it to agricultural lands in Bani Hushaysh and the Sana'a Basin. In general, the topography of Bani Hushaysh within the Sana'a Basin contributes to the collection and storage of water, which supports local agriculture and provides water sources for the region.

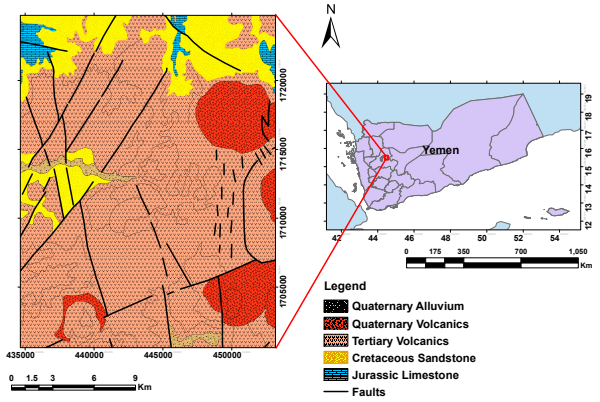

Figure 1. Shows location of the study area.

- **Geological Setting**
  As shown in (Fig. 1), the geology of the research area is mostly composed of rock successions and layers ranging from youngest to oldest.
- **Quaternary Deposit:**
  Dispersed throughout the study region and beyond, this deposit is made up of agricultural
  clay and sandy soil combined with stone fragments.
- **Quaternary Volcanic:**
  Northwest of the basin, a plateau of massive basalt cones interlayered with tuffs and alluvial sediments was formed by volcanic activity that persisted into the Quaternary. The Quaternary basalts comprise over

20% of the basin's total area and range in thickness from 100 m to 300 m.

- **Tertiary Volcanic:**
  Approximately 35% of the Sana'a Basin is covered by tertiary volcanic rock. They underlie the quaternary deposits in the southern part of the Sana'a Basin and form high plateaus to the east, west, and south of the basin. It consists of mixed basalt flows and rhyolite lavas as well as basalts, tuffs, and pyroclastic interbedded with fluvial-lacustrine deposits and thick, homogeneous basalt flow with columnar jointing. The overall thickness varied, making it difficult to estimate the level of groundwater contamination. Pollutants from the ground surface have the potential to diffuse and percolate into the groundwater system. These rocks constitute the research area and its environs.
- **Tawilah Group (Cretaceous):**
  It is made up of many medium-to coarse-grained continental cross-bedded sandstones that are occasionally silty, mudstones, and interbedded siltstones. Cretaceous sandstone covers almost 15% of the basin's total area in the northern and northeastern regions of the basin. It is believed to be between 400 and 850 m thick. The primary aquifer in the area was formed by Cretaceous sandstone. Its permeability is modest throughout the region, but it is locally higher in areas that have weathering and fractures. In the south of the basin, hundreds of meters of Tertiary volcanic rock enclose the sandstone. These rock outcrops, which are situated in Wadi Al-Sir and Wadi Rajam to the west of the study region, are distinguished by their groundwater saturation.
- **Amran Group (Middle to Upper Jurassic):**
  Dolomite and limestone were also found in the Amran Group. It encompasses 15% of the northern outcrops of the basin. Although supplies can be obtained from the zones of secondary permeability, Amran limestone is typically regarded as a weak aquifer. This group is dispersed north of the research area in the Nihm district. The structural composition of the Sana'a Basin has been thoroughly examined in only a few studies, based on seismic and drilling data. The basin has more complex structural tendencies that are presently experiencing extremely active marine floor spreading (the Gulf of Aden to the south, the Zagrous thrust to the east, the Dead Sea strike-slip fault to the north, and the Red Sea to the west). The primary tectonic tendencies and key structural elements are indicated by these borders, where a deep depression was formed by the NW-SE trend. The Sana'a Basin exhibits distinct tectonic trends of compressional and extensional regimes, as shown in Figure 1 and Table 1, [7]. The exposed rocks of the research area display a wide variety of surface tectonic features of different lengths, types, and trends (Fig. 1), suggesting that the region, as well as the Arabian Peninsula and Yemen, are subject to recurring cycles of tectonic activity. Three different fault types split the Precambrian rocks; the oldest of these, which runs parallel to the oldest Precambrian Orogeny structure, are the E–W and ENE–WSW trending faults [8]. In addition to the minor trend NNW–SSE parallel to the Red Sea, the second type is more recent and is characterized by tension faults directed in the NW–SE direction (i.e., parallel to the Najd fault trend) and occasionally reactivated [7]. Yemen's tectonic development was governed by two major tectonic eras. Several rift basins formed as a result of the initial events that occurred during the Late Jurassic–Early Cretaceous. The second was associated with the Arabian Peninsula's collision with Eurasia and the opening of the Red Sea and Gulf of Aden, respectively [9]. A number of rift basins across Yemen from west to east were created by the Late Jurassic rejuvenation of the late Proterozoic NW–SE Najd fracture system. The internal rifts of the central and western regions follow the Najd trend and are aligned NW-SE. They are progressively more east-west oriented toward the east [10, 11]. According to Al-Khanbari (2020), Yemen may be split into six seismic zones, with four seismic regions encompassing the continental portion of Yemen and two main regions around the Red Sea Mountain range and Gulf of Aden, which represent the most active locations. The Yemeni land is the most active area in the west. He added that a crack in the upper crust caused by rock stretching since the Tertiary period was the main cause of seismic activity in the volcanic margin (west of Yemen). Yemen, which is included in the study area, is therefore inside an active tectonic setting because the western seismic region has the highest level of seismic risk, whereas the central and eastern regions have minimal risk [12].

2. MATERIALS AND METHODS

Aeromagnetic surveys, conducted from aerial platforms, are essential in geophysical studies for mapping magnetic anomalies and understanding subsurface geological structures. Known for their high accuracy and cost-effectiveness, they are widely used in mineral exploration, environmental studies, and geological mapping [13–16].

The datasets used for this investigation comprised the relevant prior studies on the area as well as aeromagnetic and surface geology maps (sheet 13G, 1:250,000) encompassing the study area. Oasis Montaj Geosoft V.8.3, ArcGIS V.10.6.1, RockWorks-17, and Geomatica-20 are among the programs used in this investigation. Robertson Group PLC created the Yemeni Ministry of Oil and Mineral Resources' total intensity aeromagnetic maps in 1991 using data that were continuously collected at both constant terrain clearance and constant

Table 1. Shows the type, coordinates, and directions of the geological structure in the Bani Hushaysh area, [7].

No	Type of structure	Coordinates				Direction
		Start point		End point		
		X	Y	X	Y	
1	Fault	433026	1713585	432475	1716310	NW – SE
2	Fault	431866	1713484	431670	1714136	NW – SE
3	Fault	432417	1713412	432065	1714295	NW – SE
4	Fault	432642	1708760	432765	1709960	NE – SW
5	Fault	431620	1714306	431241	1714513	NW – SE
6	Fault	430866	1719497	429964	1715528	NW – SE
7	Fault	431100	1704703	432069	1705283	N – S
8	Fault	424143	1712659	424138	1710450	NE – SW
9	Fault	421412	1719613	432177	1716972	NE – SW
10	Fault	425809	1709582	431417	1709920	NW – SE
11	Fault	432594	1706819	429122	1705830	NW – SE
12	Fault	433854	1719126	432778	1719378	N – S
13	Fault	421912	1707326	420709	1707601	NW – SE
14	Fault	430493	1714588	430468	1716249	NW – SE
15	Fault	431803	1719458	430684	1719669	NW – SE
16	Fault	423941	1706283	425059	1703936	NW – SE
17	Fault	423897	1707902	421129	1708123	NW – SE
18	Fault	431973	1710398	432860	1709823	NW – SE
19	Fault	432593	1712470	432940	1710543	NW – SE
20	Fault	436985	1718635	437397	1715207	NW – SE
21	Fault	443012	1716634	439843	1711414	NE – SW
22	Fault	425233	1727720	427470	1715367	NE – SW
23	Fault	432150	1715842	431576	1719274	NW – SE
24	Fault	438827	1714833	438674	1715865	NW – SE
25	Fault	429797	1716824	430201	1710540	NW – SE
26	Fault	429005	1712559	429478	1710539	NW – SE
27	Fault	429007	1719522	429375	1718690	N – S
28	Fault	433066	1712718	437519	1709645	NW – SE
29	Fault	431763	1712147	431897	1713836	NW – SE
30	Fault	438691	1713687	438241	1712397	SW – NE
31	Fault	441379	1715081	439280	1711483	NE – SW
32	Fault	432060	1714960	431503	1714560	NW – SE
33	Fault	433940	1714408	432110	1712806	NE – SW
34	Fault	439395	1717350	437676	1710470	NW – SE
35	Fault	436921	1717435	434877	1713896	NE – SW
36	Fault	429910	1711690	428347	1713687	SW – NE
37	Fault	429941	1716752	428241	1711633	NE – SW
38	Fault	435043	1723040	432148	1721045	NE – SW

barometric altitude. A grid with a 1-km spacing was produced after the International Geomagnetic Reference Field was removed and leveled. The constant terrain clearance dataset was extended to 100 m and the constant barometric altitude dataset to 3,350 m before contouring (with a 10 nT contour interval). Contours on the scale of 1:250,000 represent the total magnetic field map prepared by Robertson Group PLC for the Yemeni Joint

Project for Natural Resources [17]. It was acquired at a flight elevation of 3350 m with a contour interval of 50 nT, 100-m constant terrain clearance, and 3,350-m constant barometric altitude. A dividing line divides the outlines of the two datasets (Fig. 2). The aeromagnetic map of the research region was digitized at intervals of 5 km, saved in an ASCII file using an XYZ format, and gridded using the kriging method with a cell size of 100 m to overcome the challenge of elevation differences. The continuous terrain clearance dataset (located on the right side of the map) was divided into smaller parts, continued upward to 3,350 meters, and then merged with the constant barometric altitude dataset (located on the left side of the map). The entire dataset was then re-gridded, and the resulting map (Fig. 4) was used for the subsequent processing and analysis techniques, which included spectral analysis, reduction to the north magnetic pole, trend analysis, and 3D Euler deconvolution, as shown below.

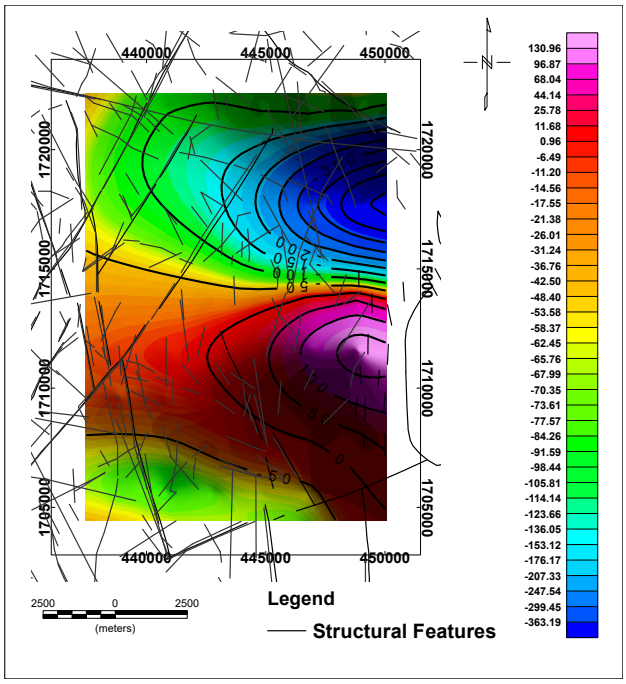

Figure 2. Total intensity aeromagnetic and Structural features map of the study area.

3. RESULTS AND DISCUSSION

- **Tectonic setting of the study area**

  Depending on the study carried out by Hydrosult of the tectonic situation of the Sana'a Basin in general and the study area in particular, the study that they carried out of the surface and subsurface structures through some geophysical methods and the wells that were drilled revealed the presence of a group of geological structures, which are the breaks and faults. The study showed that the faults were in several directions. However, the two main directions in the study area were (NE) and (NW), which represent the main direction of the study area, as its direction coincides with the opening of the Red Sea, while the faults (NE) coincide with the opening of the Gulf of Aden [7]. Structural maps of the study area were studied and analyzed, and the coordinates and length of each structure and the directions of their dipping were determined using ***ArcGIS*** and ***Geomatica-20*** programs, and then the ***RockWorks-17*** program was used to find out the direction of the faults or structures affecting the study area. The results of this study were divided into two parts.

1- The first part (**NW – SE**): These are the faults that have the main influence in the study area, and the main reason for their formation was the Najd fault, as these faults were reactivated by the opening of the Red Sea.

2- The second part (**NE – SW**): These are the faults that have a major influence in the study area, but come after the faults of the first part, as they are affected by the expansion of the Gulf of Aden. As the Arabian plate diverges from the Somali plate in the Gulf of Aden, lateral forces are formed that affect the region and cause the faults to head towards the northeast. This divergence creates lateral pressure forces that lead to the formation of faults towards the NE due to the distribution of tectonic forces between the Red Sea and the Gulf of Aden, as the two plates play a role in reactivating the faults that tend towards the northeast.

- **Processing and interpretation of aeromagnetic data**

  The process of processing magnetic anomalies involves analyzing digital data to improve the subsurface image obtained by making the magnetic anomaly signals clearer. The current study employed several processing and interpretation methods such as spectrum frequency analysis, reduction to the north magnetic pole, separation of residual and regional magnetic anomaly components, and Euler deconvolution.

- **Reduction to the north magnetic pole**

  In regions with low-to-moderate magnetic latitudes, the technique of reducing magnetic anomalies to the magnetic pole is commonly utilized to simplify the interpretation of magnetic data and improve its correlation with geological maps. By repositioning the peaks of these anomalies closer to their original centers, this method effectively reduced distortions and streamlined the interpretation process. Figure 5 presents the reduced-to-pole (RTP) map, illustrating the cumulative effects of magnetic susceptibility from various rock types and geological structures, with variations in depth from subsurface levels to the Earth's surface. An overview of the map indicates that prominent positive magnetic anomaly features are located in the

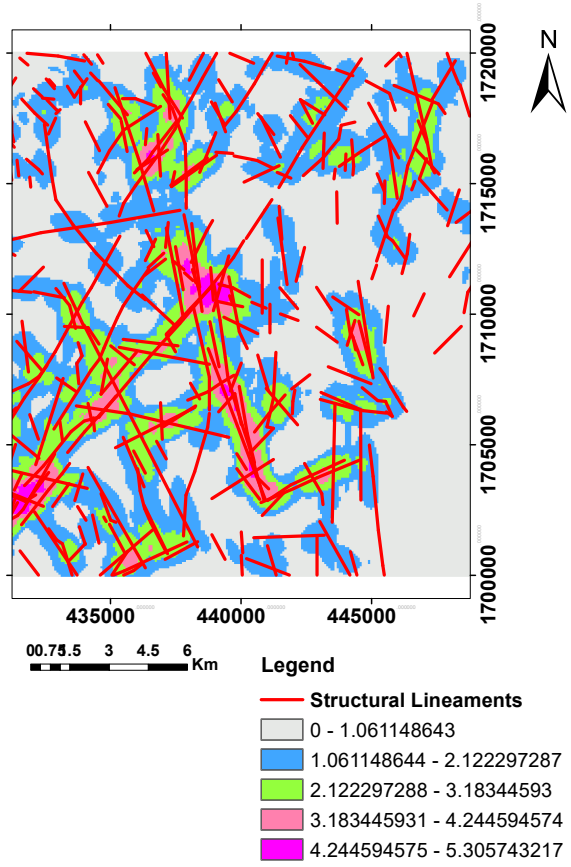

Figure 3. Map shows the density of geological structures in the study area.

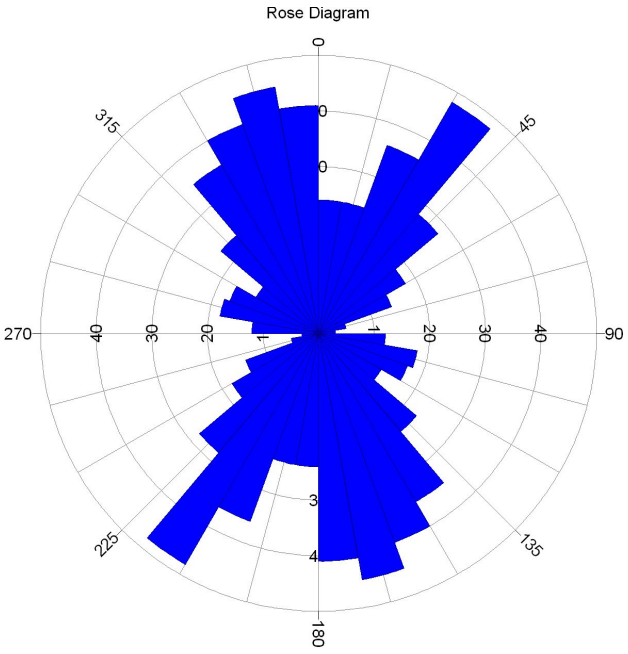

Figure 4. Rose diagram shows the directions of faults in the study area.

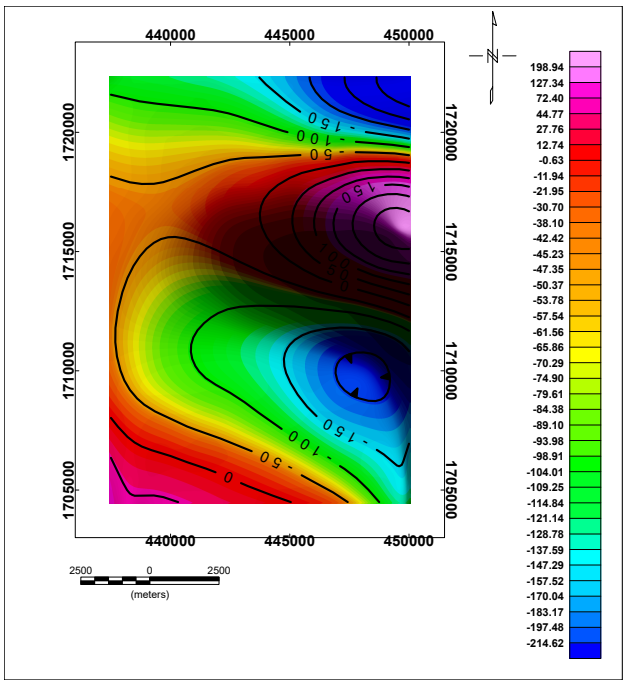

Figure 5. Reduced to the pole (RTP) aeromagnetic map of the study area.

upper section, particularly in the northeastern area, extending at a relatively oblique angle from the NE to the NW. This region contained a significant positive anomaly closure with a maximum amplitude of 200 nT. In addition, minor positive magnetic anomaly features were observed in the southern part of the map, specifically in the southwestern section, with a maximum amplitude of 50 nT. Conversely, substantial negative magnetic anomaly features were found in the northeastern part of the map, comprising major negative magnetic anomaly features present in the northeastern section, with a minimum value of -200 nT. Minor negative anomaly closure with a minimum value of -150 nT, extending at an oblique angle from the southeast to northwest. Given the small and limited study area, these findings highlight the constrained characteristics of both the positive and negative magnetic anomalies, as demonstrated by the observed closures.

- **Separation of magnetic anomaly components**

The main goal of this procedure is to separate the long-wavelength (regional) and short-wavelength (residual) magnetic anomalies. Based on the radially averaged power spectrum curve, the cutoff wavelength utilized in the filter design must be precisely selected for this separation to be successful. Figure 6 shows the 2D power spectrum of the RTP map for the research area. Two primary spectral components can be identified in the spectrum curve based on the shift in the spectral decay rate. The average depths to the top of the corresponding anomaly sources were estimated using the slopes of the best-fit linear segments

of these spectral components [18]. The average depth of the magnetic anomaly sources was calculated to be 3.086 km for the deep anomaly sources and 1.698 km for the shallow anomaly sources. The radial spectrum curve Figure 6 shows that the boundary between the regional and residual magnetic anomalies is represented by wave number (k) = 0.25. To separate the components of the magnetic anomaly, Butterworth low-pass and high-pass filters (k = 0.25), as well as bandpass filters (k = 0.08 – 0.25 and k = 0.25 – 0.4), were used, with the regional anomalies coming first, followed by the residual anomalies.

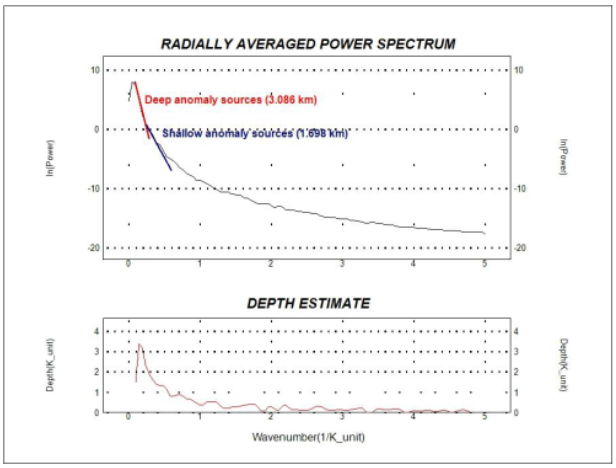

Figure 6. 2D radially averaged power spectrum of magnetic data for the study area.

- **Residual magnetic anomaly map**
  A belt-shaped arrangement of high-resolution, high-frequency magnetic anomalies can be observed on the residual anomaly map (Fig. 7). Connected rounded closures with various frequencies and amplitudes make up for these anomalies. The existence of faults or geological contacts that split the examined area into discrete blocks, each with unique magnetic properties, is suggested by the fluctuation between positive and negative anomalies as well as by sharp gradients and elongated structures. This anomalous belt mostly runs NW-SE, following major faults that impact the area, especially as these rifts line up with regions related to the development of the Red Sea and the Gulf of Aden. Because of the limited size of the study region, other directional trends were less noticeable in this orientation, although the upper portion of the map was more noticeable. This map's lateral movement of positive and negative magnetic closures in various directions is a noteworthy feature that suggests that the area has experienced many episodes of residual and regional tectonic activity. Negative anomalies are categorized as subsided formations (such as grabens and synclines) in the SE direction up to -35nT, while positive magnetic closures are understood as uplifted structures (such as horsts and anticlines) in the NE direction up to 35nT. Moreover, the correlation between the residual map's magnetic anomalies and the region's topographic and geological maps revealed that the majority of positive and negative magnetic anomalies corresponded to high and low topographic features, respectively. Furthermore,some anomalies were linked to variations in the magnetic susceptibility of nearby rock units in the area.
- **Regional magnetic anomaly map**
  The map depicting deep or regional magnetic anomalies in the study area (Fig. 8) were distinguished by low-frequency patterns that were smooth and took on rounded and elongated shapes. Mostly oriented NE-SW–SW structures created alternating bands of positive and negative magnetic anomalies. Significant deep faults are likely to be present in the regions surrounding the positive magnetic anomalies, as evidenced by their notable abrupt gradients. There are notable similarities between the RTP and regional magnetic maps in terms of the alignment and distribution of the high- and low-magnetic zones across the mapped area. Additionally, some of the anomalies seen on the RTP map come from deeper geological processes because they appear as large, solitary anomalies with reduced amplitudes and frequency on the regional map. This approach emphasizes the importance of deep-seated geological formations in the formation of the region's tectonic landscape. A notable difference in geological features is further shown by the fact that the total magnetization of rocks at the surface and near-surface levels is significantly lower than that of deeper rock formations.
- **Structural lineament interpretation**
  Mapping structural trends by tracking lineation in magnetic contours is one of the most practical geological uses of magnetic surveys. This is because these lineations depict the tectonic events affecting the nation rocks and reflect the subsurface geological conditions in such a way that the distinctive features of a particular anomaly set are connected to certain functions of the total impacting stresses [19]. The purpose of this study is to determine the prevailing tectonic trends in the area and then determine residual and regional anomaly maps as well as lines derived from the RTP (Figs. 1, 5, 7, and 8) and then analyze and study them considering the azimuth and longitude angles and display them in the form of rose diagrams. As shown in Figure 4 and 10, the NW direction represents the main direction of the faults distributed throughout the study area, most of which are concentrated in the western regions and are largely associated with volcanic rocks dating back to the modern Cenozoic era, which cover the northwestern part of the study area (Fig. 1). A secondary direction was also observed on the map,

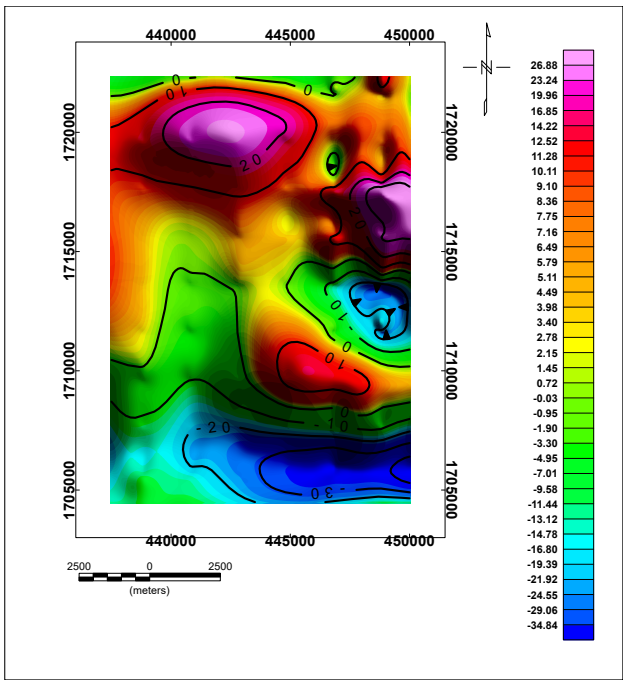

Figure 7. Residual magnetic anomaly map of the study area.

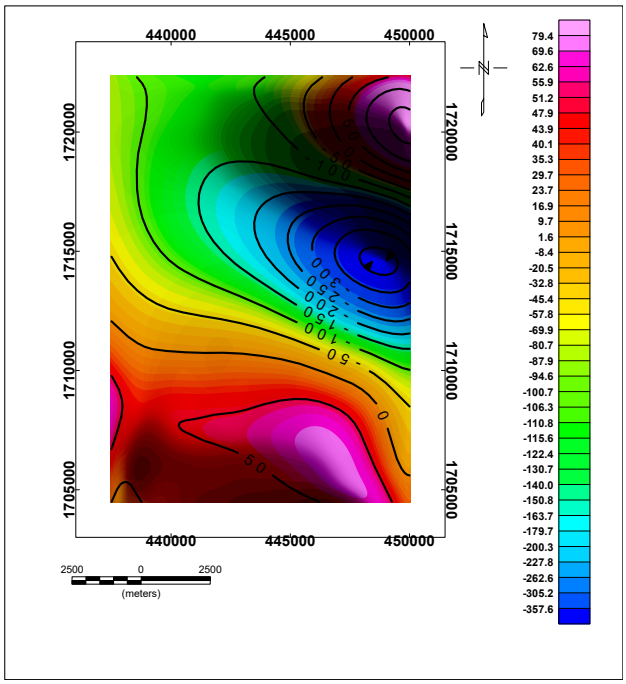

Figure 8. Regional magnetic anomaly map of the study area.

which is the NE direction, which is associated with the opening of the Red Sea and the Gulf of Aden, as the area is covered by sandstone rocks within the Tawila Group, whose geological age dates back to the Cretaceous of the Mesozoic era. From Figure 9A and Table 2, it is clear that the NE direction is the main direction, and its distribution appears throughout the map, but it prevails in the central and northern parts, which is tectonically related to volcanic activities in the region during the Cenozoic era. There are also secondary directions represented by the NW direction related to the same direction of the Najd Rift System, which is believed to have been reactivated by the opening of the Red Sea and Gulf of Aden. As shown in Figures 9B & 10, and Table 2, the NE direction represents the main direction, which may be related to the tectonic activity that caused the opening of the Red Sea and the Gulf of Aden; however, in the NW direction, a number of faults are distributed throughout the region and are tectonically affected by what happened in the Cenozoic era, as faults from this system prevail in an east-west direction.

The structural directions recorded in this map (Fig. 9C and Fig. 11) are related to the tectonic activity that affected the country during the Paleozoic era, from which the Sana'a Basin was formed. The Cenozoic era created many rift basins and sub-basins in different directions, and the location of Volcanoes in Yemen opened the Gulf of Aden and Red Sea. The map revealed that the directions are mainly NW and northeast throughout the region, with volcanic rocks dating back to the Cenozoic era spread in the northwestern parts. Sandstone rocks belonging to the Tawilah group within the Mesozoic era are also widespread. At the end of this discussion, the following remarks can be drawn: The trend information obtained through the local magnetic anomaly maps and structural lines interpreted from the RTP shows that the unfolding structural trends from the surface geological map are consistent with the interpretation derived from the magnetic anomaly maps, but with some minor differences, such as the difference in the azimuth angle. We can also say that the change in trends is caused by tectonic tension and compression factors throughout the geological history of the magnetic field in the study area. The northwest direction is the most common structural direction, and the NE direction is considered a secondary structure associated with the reactivation of the Najd fault system, during which several rift basins formed during the Mesozoic, while its reactivation was associated with the development of volcanoes during the Cenozoic.

- **Euler deconvolution**

Geologic connections were delineated by depth estimation using the Euler deconvolution approach. This method automatically calculated the depth and location of the source. Therefore, Euler deconvolution is a technique for both depth estimation and boundary finding. Because it requires no information on the magnetization vector and, more crucially, only a small amount of prior knowledge regarding the magnetic source geometry, Euler deconvolution is frequently used in magnetic interpretation [20, 21]. Euler's homogeneity equation 1 must be solved to perform Euler deconvolution [21].

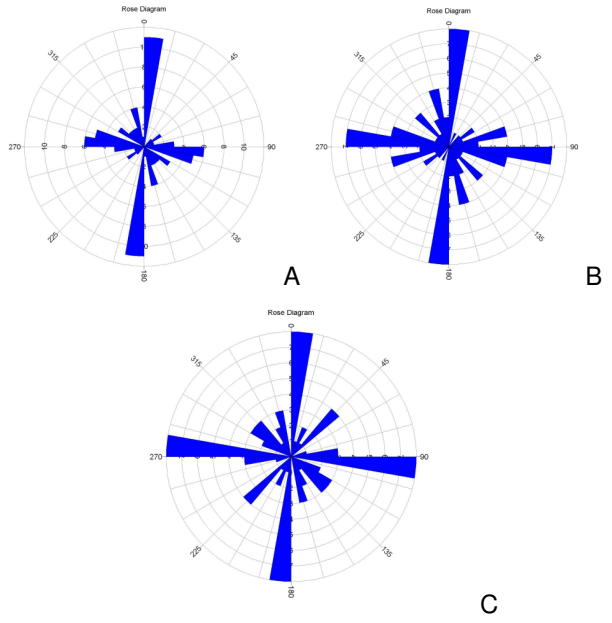

Figure 9. Rose diagrams of the traced magnetic lineaments from RTP (A) and residual, and regional magnetic anomaly maps (B and C) respectively.

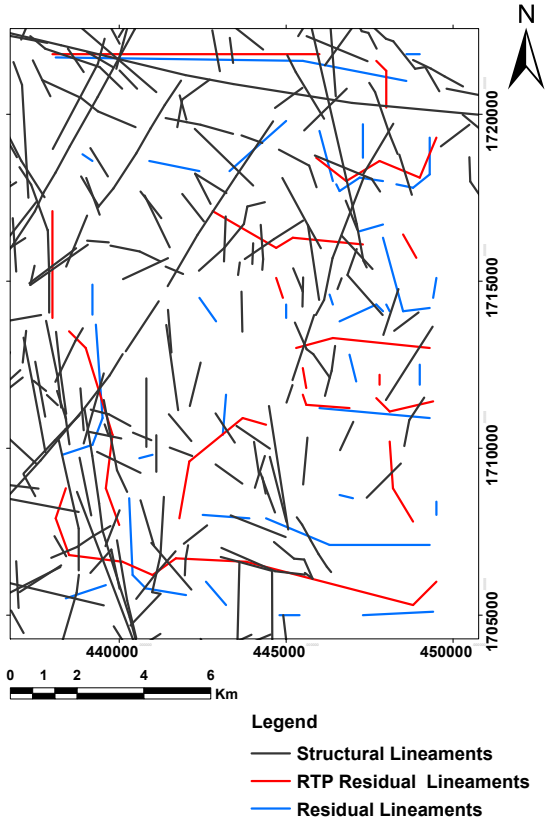

Figure 10. Lineament from surface geological and residual aeromagnetic anomaly map.

$$(x-x_0)\frac{\partial M}{\partial x}+(y-y_0)\frac{\partial M}{\partial y}+(z-z_0)\frac{\partial M}{\partial z}=N(B-M) \quad (1)$$

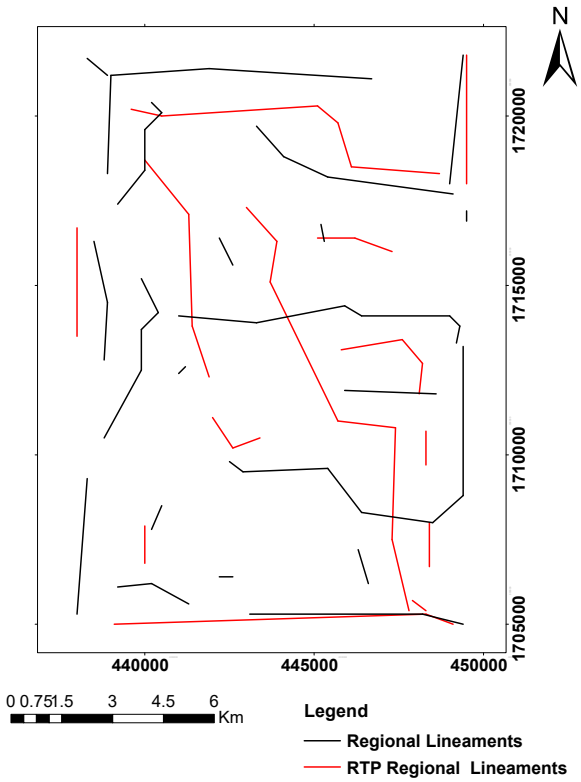

Figure 11. Lineament map derived from the RTP and regional aeromagnetic anomaly maps.

Table 2. the different structural trends deduced from the rose diagrams.

Map name	Major trend	Intermediate trend	Minor trend	Mean trend
Geological map	N30-40E	N10-20W N30W N30-40W N20-30E N40-50E N20E	N40-50W N60-85W N45-75E	N35W
RTP magnetic anomaly map	N0-15E	N10-20W N70-90W	N15-60W N0-15W, N45-90E	N80E
Residual magnetic anomaly map	N0-15E	N70-90W N10-20W N70-80E	N40-50W N0-30W, N30-70W N45-70E N80-90E,	N75E
Regional magnetic anomaly map	N0-15E N75-90W	N40-50E N80-90E N10-20W N40-50W	N25-40W, N60-70W N10-40E, N70-80E	N45W

where (x_0, y_0, z_0) is the location of the magnetic source that generates the total magnetic field M measured at (x, y, z) and B is the regional value of the total magnetic

field. N is the structural index. The position and depth of the sources were determined by solving an overestimated system of linear equations for each shifting window position [20, 21]. Thus, we can estimate the shape and depth of the magnetic sources by varying N. It has been demonstrated that poor structural index selection results in significant biases in depth estimates, as well as a diffuse solution of source locations. A proper N provides the tightest clustering of Euler solutions around the geologic structure of interest, according to both Thompson (1982) [20] and Reid et al. (1990) [21]. Physically conceivable N values for the magnetic data fall between 0 and 3. An efficient vertical line source, such as a narrow vertical pipe, produces an inverse square field fall-off and an index of 2, whereas the magnetic field of a point dipole falls off as an inverse cube, providing an index of 3. A field strength that grows with the distance from the source (and is infinite at infinity) is implied by values smaller than zero. The residual map and RTP for the total intensity aeromagnetic field have both been subjected to the Euler approach. The Standard Euler 3D method of the Geosoft package software V.8.3 was used to perform Euler deconvolution on the study area. The Standard Euler 3D technique is based on Euler's homogeneity equation, which uses a structural index to relate the source position to the magnetic field and its gradient components ($\frac{\partial M}{\partial x}$, $\frac{\partial M}{\partial y}$ and $\frac{\partial M}{\partial z}$) computed in the frequency domain). The system calculates the anomaly position, depth, and base level for a particular magnetic source by simultaneously solving Euler's equation for each grid position inside a window using the least-squares method. Good clustering of solutions is shown by the interpretation of Euler solutions computed using N=0.0 with 10% depth uncertainty (Fig. 12), suggesting that the anomalous sources are primarily located near the fault and contact-like structures. These solutions also exhibited excellent clustering with anomaly sources interpreted from the residual magnetic anomaly map (Fig. 13). At depths <500 m, they are primarily distributed along the edges of the magnetic anomaly sources, whereas at depths of 750–1000 m, a dense clustering of solutions (in the range <250–850 m) occurs in the northwest and southeast. Particularly, above the centroid of the positive and negative magnetic anomaly sources, the Euler solution clusters are dispersed throughout the 250–1000 m range.

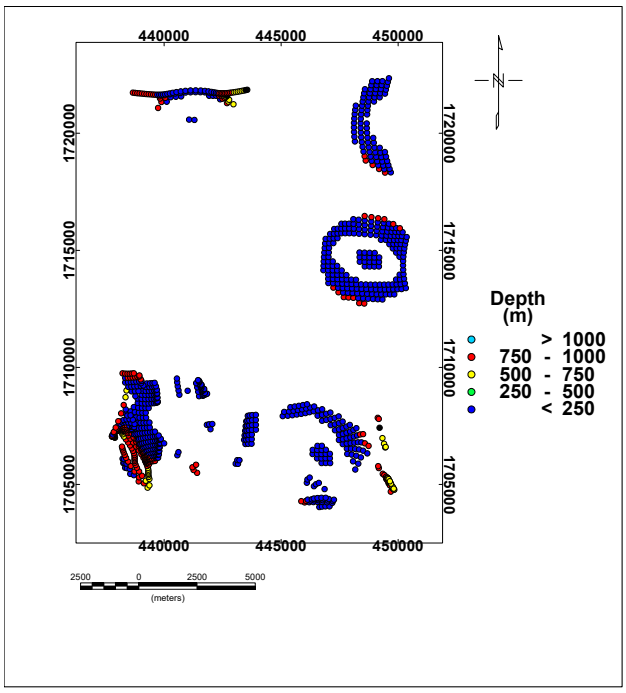

Figure 12. Euler solutions for RTP aeromagnetic anomaly map.

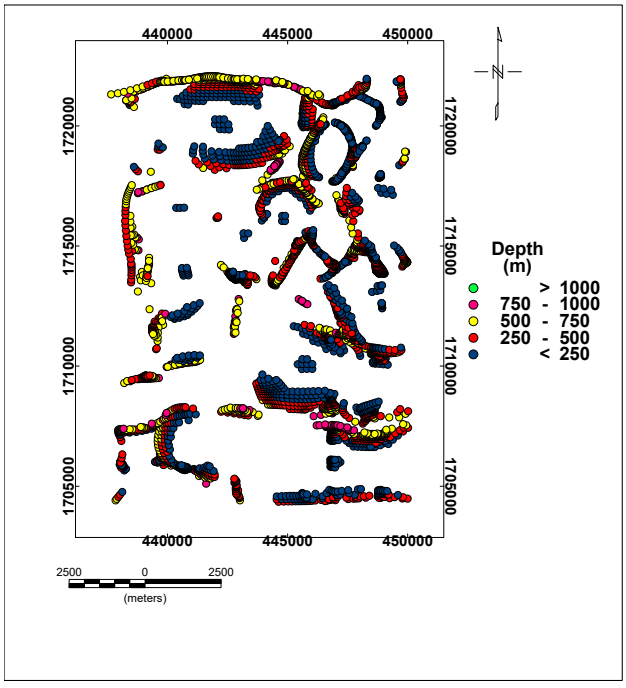

Figure 13. Euler solutions for residual aeromagnetic anomaly map.

4. CONCLUSION

- The study area has experienced several cycles of tectonic activity throughout its geological history, which has shaped its structural framework. The Najd Rift System (NW-SE), originating from the Late Precambrian, is a significant tectonic feature. Its reactivation led to the formation of the Yemeni volcanoes, the development of rift basins such as the Sana'a Basin during the Paleozoic, and the opening of the Red Sea during the Cenozoic, which further reactivated these faults.
- The residual magnetic anomaly map revealed a prominent NE-SW trend associated with the opening of the Gulf of Aden during the Cenozoic, indicating possible reactivation of ancient Precambrian orogenies. Distinct magnetic anomaly zones were observed in

the northeastern and southeastern parts of the study area, which correspond to shear zones with similar characteristics. The depths of the magnetic anomaly sources range from less than 250 m to 3000 m, with the main depth between less than 250 m and 1000 m.

REFERENCES

[1] A. Al-Subbary, A. Al-Kotbah, N. Abu-Lohom, and A. Al-Asadi, "Stratigraphic sequence and structural evolution of the sana'a basin," *Thamar Univ. J. Nat. & Appl. Sci.*, vol. 4, no. 1, pp. 49–65, 2011.

[2] A. Yahia and M. Bouabid El, "Assessment of aquifer vulnerability based on gis and arcgis methods: A case study of the sana'a basin (yemen)," *J. Water Resour. Prot.*, vol. 2011, 2011.

[3] P. Betts, R. Armit, C. Tiddy, S. Armistead, and L. Aillères, "Tectonic analysis of regional potential field data," in *Proceedings of the Australian Exploration Geoscience Conference (AEGC)*, Perth, Australia, 2019, pp. 1–5.

[4] R. J. Blakely, *Potential theory in gravity and magnetic applications*. Cambridge university press, 1996.

[5] W. H. Mohamed, M. H. Elyaseer, and M. E. M. Sabra, "Structural lineament analysis of the bir el-qash area, central eastern desert, egypt, using integrated remote sensing and aeromagnetic data," *Sci. Reports*, vol. 13, no. 1, p. 21 569, 2023.

[6] A. Tzanis, H. Kranis, and S. Chailas, "An investigation of the active tectonics in central-eastern mainland greece with imaging and decomposition of topographic and aeromagnetic data," *J. Geodyn.*, vol. 49, no. 2, pp. 55–67, 2010.

[7] Hydrosult, "Aquifer storage investigations and assessment: Assessment of the water resources of the sana'a basin strategic options for the sustainable development of the basin's water resources," 2007.

[8] Z. Beydoun *et al.*, "International lexicon of stratigraphy," *Vol. III, Repub. Yemen, second edition: international union geological sciences ministry oil mineral resources, Repub. Yemen publication*, vol. 34, p. 245, 1998.

[9] I. Csato, "Extensional tectonics and salt structures, marib-shabwa basin, yemen," in *AAPG Annual Convention, Dallas*, Citeseer, 2005, pp. 1–6.

[10] Z. R. Beydoun, *Arabian plate hydrocarbon geology and potential—a plate tectonic approach*. American Association of Petroleum Geologists, 1991.

[11] Z. R. Beydoun, "Introduction to the revised mesozoic stratigraphy and nomenclature for yemen," *Mar. Petroleum Geol.*, vol. 14, no. 6, pp. 617–629, 1997.

[12] K. Khanbari, "Seismotectonic provinces of yemen," *J. Sci. Space Technol.*, vol. 6, no. 8, 2020.

[13] I. Kiani and R. Okosiemiema, "Reviewing the art of aeromagnetic data interpretation in geophysical surveys.," *Fac. Nat. Appl. Sci. J. Sci. Innov.*, vol. 5, no. 2, pp. 38–43, 2023.

[14] P. G. Betts *et al.*, "Geology from aeromagnetic data," *Earth-Science Rev.*, p. 104 958, 2024.

[15] B. Gavazzi, L. Bertrand, M. Munschy, J. Mercier de Lépinay, M. Diraison, and Y. Géraud, "On the use of aeromagnetism for geological interpretation: 1. comparison of scalar and vector magnetometers for aeromagnetic surveys and an equivalent source interpolator for combining, gridding, and transforming fixed altitude and draping data sets," *J. Geophys. Res. Solid Earth*, vol. 125, no. 5, e2019JB018870, 2020.

[16] N. C. White, *Geological interpretation of aeromagnetic data (david j. isles and leigh r. rankin)*, 2014.

[17] M. of Oil and T. N. R. P. (Minerals, *Aeromagnetic map of yemen sheet 13g*, 1991.

[18] A. Spector and F. Grant, "Statistical models for interpreting aeromagnetic data," *Geophysics*, vol. 35, no. 2, pp. 293–302, 1970.

[19] M. B. Dobrin and C. H. Savit, *Introduction to Geophysical Prospecting*, 4th. New York: McGraw-Hill, 1988, p. 741.

[20] D. Thompson, "Euldph: A new technique for making computer-assisted depth estimates from magnetic data," *Geophysics*, vol. 47, no. 1, pp. 31–37, 1982.

[21] A. B. Reid, J. Allsop, H. Granser, A. t. Millett, and I. Somerton, "Magnetic interpretation in three dimensions using euler deconvolution," *Geophysics*, vol. 55, no. 1, pp. 80–91, 1990.